

See discussions, stats, and author profiles for this publication at: <https://www.researchgate.net/publication/228097547>

# Ab Initio Search for Ditopic Silene Complexes with Methylene-Bridged Ligands Containing Both Donor and Acceptor Sites

## Ab Initio Search for Ditopic Silene Complexes with Methylene-B...

ARTICLE in ORGANOMETALLICS · FEBRUARY 2009

Impact Factor: 4.13 · DOI: 10.1021/om800243j

---

CITATIONS

2

---

READS

119

6 AUTHORS, INCLUDING:



Vitaly Avakyan

Russian Academy of Sciences

84 PUBLICATIONS 385 CITATIONS

SEE PROFILE



Valery F. Sidorkin

Irkutsk Institute of Chemistry of the Russia...

48 PUBLICATIONS 300 CITATIONS

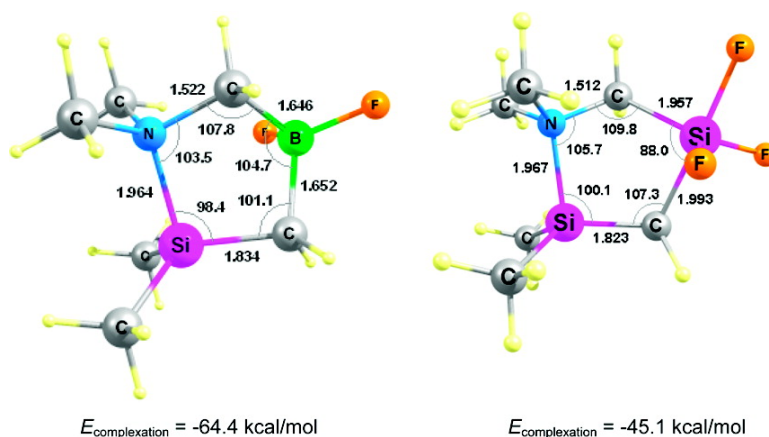
SEE PROFILE

## Ab Initio Search for Ditopic Silene Complexes with Methylene-Bridged Ligands Containing Both Donor and Acceptor Sites

Vitaly G. Avakyan, Stephan L. Guselnikov, Valery F. Sidorkin, Evgeniya P. Doronina, and Leonid E. Gusel'nikov

*Organometallics*, 2009, 28 (4), 978-989 • DOI: 10.1021/om800243j • Publication Date (Web): 21 January 2009

Downloaded from <http://pubs.acs.org> on March 17, 2009



### More About This Article

Additional resources and features associated with this article are available within the HTML version:

- Supporting Information
- Access to high resolution figures
- Links to articles and content related to this article
- Copyright permission to reproduce figures and/or text from this article

[View the Full Text HTML](#)



ACS Publications  
High quality. High impact.

Organometallics is published by the American Chemical Society, 1155 Sixteenth Street N.W., Washington, DC 20036

# Ab Initio Search for Ditopic Silene Complexes with Methylene-Bridged Ligands Containing Both Donor and Acceptor Sites

Vitaly G. Avakyan,<sup>†,‡</sup> Stephan L. Guselnikov,<sup>\*,†</sup> Valery F. Sidorkin,<sup>§</sup>  
Evgeniya P. Doronina,<sup>§</sup> and Leonid E. Gusel'nikov<sup>†</sup>

Topchiev Institute of Petrochemical Synthesis, Russian Academy of Sciences, 119991 GSP-1, Moscow, Russian Federation, Photochemistry Center, Russian Academy of Sciences, 117421 Moscow, Russian Federation, and A. E. Favorsky Irkutsk Institute of Chemistry, Siberian Branch of the Russian Academy of Sciences, 664033, Irkutsk, Russian Federation

Received September 21, 2007

Complexation of ditopic ligands  $\text{Me}_2\text{N}(\text{CH}_2)_n\text{X}$  ( $n = 0-2$ ;  $\text{X} = \text{BF}_2, \text{SiF}_3$ ) containing both donor and acceptor sites was studied at the MP4/6-311G(d,p)/MP2/6-31G(d,p)+ZPE level of theory to estimate their capability of simultaneously binding to both ends of silenes,  $\text{R}_2\text{Si}=\text{CH}_2$  ( $\text{R} = \text{H}, \text{Me}$ ), to give cyclic complexes. Predicted to be stable were the ditopic complexes **7** and **8** of the parent silene and 1,1-dimethylsilene with methylene-bridged ligands ( $n = 1$ ) formed by both  $\text{N} \rightarrow \text{Si}$  and novel dative bonds of silenic carbon to boron ( $\text{C} \rightarrow \text{B}$ ) or silicon ( $\text{C} \rightarrow \text{Si}$ ) with complexation energies reaching  $-64.4$  kcal/mol. However, all efforts to optimize complexes with ligands containing no or two methylene groups ( $n = 0$  or  $2$ ) resulted in insertion products **3** and **5**. The nature of the bonding in the ditopic complexes is discussed in terms of structural and energetic parameters, supported by the data from the AIM and ELF topological analyses.

## Introduction

Nonhindered silenes are kinetically, not thermodynamically, unstable compounds appearing as reactive intermediates in various thermal and photochemical reactions occurring in the gas and liquid phases.<sup>2</sup> Their instability is due to the extremely high reactivity toward formation of cyclodimers (1,3-disilacyclobutanes). The cyclodimerization can be suppressed by generating silenes in the gas phase under very low pressure or by isolation in solid matrixes. Protection of silenes against cyclodimerization can be attained by (i) introducing sterically hindered substituents,<sup>3</sup> (ii) reducing or even reversing the

polarity of the  $\text{Si}=\text{C}$  bond by the appropriate substituents,<sup>4</sup> or (iii) using the coordination potential of the electron-deficient Si of the  $\text{Si}=\text{C}$  double bond, i.e., inter- or intramolecular complexation of  $\text{sp}^2$ -hybridized silicon with  $n$ -donors.<sup>5</sup> The isolated  $n$ -donor complexes found in the literature all contain bulky substituents at the silicon and/or carbon atoms.<sup>5e</sup> Therefore, their kinetic stability is due to the contribution of factors (i), (ii), and (iii). Stabilization by factor (iii) is rationalized by the increase of the cyclodimerization barrier, which is close to 0 kcal/mol for simple silenes, and by the value of the complexation energy.<sup>2i</sup>

As predicted by ab initio study, the complexation energies of silenes,  $\text{R}_2\text{Si}=\text{CH}_2$  ( $\text{R} = \text{H}_3\text{Si}, \text{H}, \text{Me}, \text{H}_2\text{N}, \text{OH}, \text{Cl}, \text{F}$ ), with trimethylamine linearly grow to  $-37$  kcal/mol as the substituents' electronegativities increase.<sup>6</sup> A fairly high energy of intramolecular complexation was also derived for 1-methylene-5-methyl-5-aza-2,8-dioxa-1-silacycloalkane ( $-19.7$  kcal/mol) and 1,1-bis[ $N$ -(dimethylamino)acetamidato]silene ( $-26.8$  kcal/mol).<sup>7</sup> The total coordination potential of the polar and easily

\* To whom correspondence should be addressed. Tel: +7 495 952 5162. Fax: +7 495 955 4898. E-mail: guselnikovsl@ips.ac.ru.

<sup>†</sup> Topchiev Institute.

<sup>‡</sup> Photochemistry Center.

<sup>§</sup> Favorsky Institute.

(1) Partly presented: Guselnikov, S. L.; Avakyan, V. G.; Gusel'nikov, L. E. 4th European Silicon Days, September 9–11, 2007, Bath, UK, Abstracts, p 118.

(2) (a) Gusel'nikov, L. E.; Nametkin, N. S.; Vdovin, V. M. *Acc. Chem. Res.* **1975**, *8*, 18. (b) Gusel'nikov, L. E.; Nametkin, N. S. *Chem. Rev.* **1979**, *79*, 1396. (c) Raabe, G.; Michl, J. *Chem. Rev.* **1985**, *85*, 419. (d) Gusel'nikov, L. E.; Nametkin, N. S. In *Advances in Organosilicon Chemistry*; Voronkov, M. G., Ed.; Mir Publishers: Moscow, 1985; p 69. (e) Raabe, G.; Michl, J. In *The Chemistry of Organic Silicon Compounds*, Vol. 1; Patai, S.; Rappoport, Z., Eds.; Wiley: Chichester, 1989; p 1015. (f) Gusel'nikov, L. E.; Avakyan, V. G. *Soviet Scientific Reviews, Section B, Chemistry Reviews*; Vol'pin M. E., Ed.; 1989; Vol. 13, p 39. (g) Pola, J. *J. Anal. Appl. Pyrolysis* **1994**, *30*, 73. (h) Brook, A. G.; Brook, M. A. *Adv. Organomet. Chem.* **1995**, *39*, 71. (i) Muller, T.; Ziche, W.; Auner, N. In *The Chemistry of Organic Silicon Compounds*, Vol. 2; Rappoport, Z.; Apeloig, Y., Eds.; Wiley: Chichester, 1998; p 857. (j) Pola, J. *Surf. Coat. Technol.* **1998**, *101*, 408. (k) Levillain, J.; Pfister-Guillouzo, G.; Ripoll, J.-L. *Eur. J. Chem.* **2000**, 3253. (l) Gusel'nikov, L. E. *Coord. Chem. Rev.* **2003**, *244*, 149.

(3) Okazaki, R.; West, R. *Adv. Organomet. Chem.* **1995**, *39*, 232.

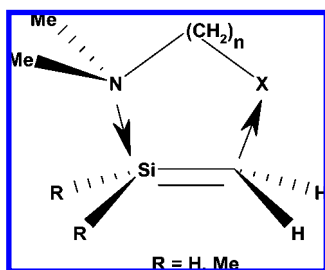
(4) (a) Apeloig, Y.; Karni, M. *J. Am. Chem. Soc.* **1984**, *106*, 6676. (b) Ottosson, H. *Chem.-Eur. J.* **2003**, *9*, 4144. (c) Bendikov, M.; Quadt, S. R.; Rabin, O.; Apeloig, Y. *Organometallics* **2002**, *21*, 3930.

(5) (a) Wiberg, N.; Joo, K.-S.; Polborn, K. *Chem. Ber.* **1993**, *126*, 67. (b) Wiberg, N.; Koepf, H. *J. Organomet. Chem.* **1986**, *315*, 9. (c) Wiberg, N.; Scurz, K. *Chem. Ber.* **1988**, *121*, 681. (d) Wiberg, N.; Schurz, K. *J. Organomet. Chem.* **1988**, *341*, 145. (e) Wiberg, N. In *Organosilicon Chemistry II. From Molecules to Materials*; Auner, N.; Weis, J., Eds.; VCH: Weinheim, 1996; p 367. (f) Avakyan, V. G.; Gusel'nikov, L. E.; Pestunovich, V. A.; Bagaturyants, A. A.; Auner, N. *Organometallics* **1999**, *18*, 4692. (g) Potter, M.; Baumer, U.; Mickoleit, M.; Kempe, R.; Oehme, H. *J. Organomet. Chem.* **2001**, *621*, 261. (h) Mickoleit, M.; Kempe, R.; Oehme, H. *Chemistry* **2001**, *7*, 987. (i) Leigh, W. J.; Li, X. *J. Am. Chem. Soc.* **2003**, *125*, 8096.

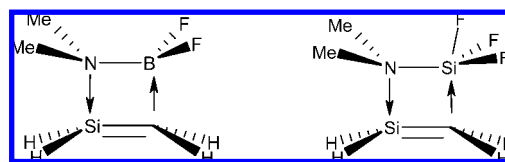
(6) Avakyan, V. G.; Gusel'nikov, L. E.; Gusel'nikov, S. L.; Sidorkin, V. F. *Izv. RAN, Ser. Khim.* **2005**, 1952.

(7) Sidorkin, V. F.; Belogolova, E. F.; Pestunovich, V. A. *Organometallics* **2004**, *23*, 2389.

Scheme 1



Scheme 2



polarizable Si=C double bond has never been used in *n*-donor complexes, as only the silicon has been involved in dative bonding, while the carbon atom, a potential electron donor, has remained uncoordinated. This prompted us to investigate interactions of simple silenes with bidentate ligands leading to silene ditopic complexes, which being more stable than the usual *n*-donor complexes might behave as convenient synthons of the silicon–carbon double bond.

Logically the search for bidentate ligands will include the following steps: (i) theoretical prediction of the most appropriate type of ligand and study of the silene–ligand system in terms of localizing the local minima on its potential energy surface (PES); (ii) theoretical investigation of the geometric and electronic structures as well as the energetics of the complex formation; and (iii) study of the reactivity of the complexes. Herein we report an ab initio study on parts (i) and (ii). We selected the ligands of the general formula  $\text{Me}_2\text{N}(\text{CH}_2)_n\text{X}$  ( $n = 0–2$ ;  $\text{X} = \text{BF}_2, \text{SiF}_3$ ) in which a nitrogen atom could donate the lone pair to an  $\text{sp}^2$ -hybridized silicon atom along with a boron- (strong acceptor) or a fluorine-substituted silicon (moderate acceptor) withdrawing the excessive electron density from the silenic carbon (Scheme 1).<sup>8</sup>

We performed (i) a successful ab initio optimization of the first ditopic silene and dimethylsilene complexes with bidentate methylene-bridged ( $n = 1$ ) ligands, formed by both  $\text{N} \rightarrow \text{Si}$  and novel coordinate bonds of silenic carbon to boron ( $\text{C} \rightarrow \text{B}$ ) or silicon ( $\text{C} \rightarrow \text{Si}$ ),<sup>9</sup> and (ii) have traced the evolution of the electron density distribution from the  $\text{Si}=\text{C}$   $\pi$ -bond to the newly formed dative  $\text{C} \rightarrow \text{X}$  bonds.

## Computational Methods

Full geometry optimization of silenes, ligands, ditopic complexes, and adducts was performed using the standard 6-31G(d,p) basis set at the MP2 level of theory.<sup>10</sup> Zero-point vibrational energies (ZPE) were determined at the same level of theory, MP2/6-31G(d,p). The hydrogen atomic mass 1.008<sup>11</sup> linearizing the

(8) For somewhat similar donor–acceptor stabilization of silaformyl compounds  $\text{R}(\text{H})\text{Si}=\text{O}$  see: Yao, S.; Brym, M.; van Wullen, C.; Driess, M. *Angew. Chem., Int. Ed.* **2007**, *46*, 4159.

(9) Dative bond is a description of covalent bonding between two atoms in which both electrons shared in the bond are coming from the same atom. Coordination occurs when an electron donor (atom possessing a lone pair, e.g., nitrogen, oxygen, etc.) donates a pair of electrons to an electron acceptor (atom possessing empty orbitals or, like silicon, having the propensity to form hypercoordinate complexes). Such a bond in the ditopic complexes is the  $\text{N} \rightarrow \text{Si}$  bond. The second dative bonds of silenic carbon to boron ( $\text{C} \rightarrow \text{B}$ ) or silicon ( $\text{C} \rightarrow \text{Si}$ ) we consider as novel ones, as they result not from the acceptance of a lone pair, which is absent for carbon, but adoption of a considerable portion of silene's  $\pi$ -electron density by boron or silicon of the ligand.

(10) (a) Krishnan, R.; Binkley, J. S.; Seeger, R.; Pople, J. A. *J. Am. Chem. Soc.* **1980**, *72*, 650. (b) Binkley, J. S.; Pople, J. A. *Int. J. Quantum Chem.* **1975**, *9*, 229. (c) Krishnan, R.; Pople, J. A. *Int. J. Quantum Chem.* **1978**, *14*, 91.

(11) Volkenstein, M. V.; Gribov, L. A.; Elyashevich, M. A.; Stepanov, B. I. *Molecular Vibration*; Nauka: Moscow, 1972 (in Russian).

difference  $\Delta\nu = \nu_{\text{calc}} - \nu_{\text{exp}}$  and the scale factor 0.96 were used when calculating the ZPE. Final energies were calculated using the fourth-order perturbation theory MP4(SDQ) for the MP2/6-31G(d,p) geometries. These single-point MP4 calculations were carried out employing an extended basis set denoted 6-311G(d,p). This basis set consists of the 6-311G(d,p) basis for the elements of the second period and hydrogen, and the McLean–Chandler (12s, 9p)/[6s, 5p](d) basis for the third period elements.<sup>12</sup> The full notation for the level of theory used is MP4(SDQ)/6-311G(d,p)//MP2/6-31G(d,p). Its use enabled us to calculate the energies of complexation with an accuracy comparable to that obtained when using standard heats of formation.<sup>13</sup> We checked the reliability of our level of theory by calculating the model donor–acceptor complex  $\text{H}_3\text{N} \cdot \text{BH}_3$ . The calculated  $\text{B} \rightarrow \text{N}$  bond energy (27.8 kcal/mol) was in a good agreement with that (25.6 kcal/mol) calculated at the higher level of theory, CCSD(T)/CCSD(T) + ZPE(MP2/aug-cc-pVTZ).<sup>14</sup> All MP2 and MP4 calculations were performed using the GAMESS suite.<sup>15</sup>

Analyses of the electron density in terms of the atoms in molecules (AIM)<sup>16</sup> theory were performed at the MP2(Full)//MP2(FC)/6-311++G(2d,p) level of theory using AIMPAC (calculation of atomic charges)<sup>16</sup> and MORPHY 1.0<sup>17</sup> program packages. The electron localization functions (ELF) of Bekke and Edgecombe<sup>18</sup> were calculated employing the TopMod program package<sup>19</sup> at the HF/6-311++G(d,p)//MP2/6-31G(d) level of theory and visualized using the GopenMol suite of programs.<sup>20</sup>

## Results and Discussion

**1.1. Attempted Modeling of Silene Complexes with  $\text{Me}_2\text{N}(\text{CH}_2)_n\text{BF}_2$  and  $\text{Me}_2\text{N}(\text{CH}_2)_n\text{SiF}_3$  ( $n = 0$  and 2) Ligands.** One can imagine that the desired silene complexes with the above ligands will be the four- and six-membered cyclic systems formed by two dative bonds, namely,  $\text{N} \rightarrow \text{Si}$ ,  $\text{C} \rightarrow \text{B}$  and  $\text{N} \rightarrow \text{Si}$ ,  $\text{C} \rightarrow \text{Si}$ , respectively, as shown in Schemes 2 and 3.

(12) McLean, A. D.; Chandler, G. S. *J. Chem. Phys.* **1980**, *72*, 5639.

(13) Gusev, L. E.; Avakyan, V. G.; Gusev, S. L. *Heteroat. Chem.* **2007**, *18*, 704, and references therein.

(14) Hernandez-Matus, M.; Grant, D.; Switzer, J.; Batson, J.; Folkes, R.; Nguyen, M.; Arduengo, A. J. [http://www1.eere.energy.gov/hydrogenandfuelcells/pdfs/storage\\_theory\\_session\\_dixon.pdf](http://www1.eere.energy.gov/hydrogenandfuelcells/pdfs/storage_theory_session_dixon.pdf).

(15) Schmidt, M. W.; Baldridge, K. K.; Boatz, J. A.; Elbert, S. T.; Gordon, M. S.; Jensen, J.; Matsunaga, N.; Nguyen, K. A.; Su, S.; Windus, T. L.; Dupius, M.; Montgomery, J. A. *J. Comput. Chem.* **1993**, *14*, 1347.

(16) (a) Bader, R. F. W. *Chem. Rev.* **1991**, *91*, 893. (b) Bader, R. F. W. *Atom in Molecules. A Quantum Theory*; Oxford University Press: New York, 1990. (c) Biegler-König, F. W.; Bader, R. F. W.; Tang, T. H. *J. Comput. Chem.* **1982**, *3*, 317.

(17) (a) Laaksonen, L. *J. Mol. Graphics* **1992**, *10*, 33. (b) Bergman, D. L.; Laaksonen, L.; Laaksonen, A. *J. Mol. Graphics Modell.* **1997**, *15*, 301.

(18) (a) Becke, A. D.; Edgecombe, K. E. *J. Chem. Phys.* **1990**, *92*, 5397. (b) Silvi, B.; Savin, A. *Nature* **1994**, *371*, 683. (c) See additional information and the literature on the ELF analysis at a legal part of the Internet website of the Max Planck Institute for the Chemical Physics of Solids (<http://www.cfps.mpg.de/ELF/>).

(19) (a) Noury, S.; Krokidis, X.; Fuster, F.; Silvi, B. *TopMod package*; Université Pierre et Marie Curie, France, 1997. (b) Noury, S.; Krokidis, X.; Fuster, F.; Silvi, B. *Comput. Chem.* **1999**, *23*, 597.

(20) (a) Popelier, P. L. A. *Comput. Phys. Commun.* **1996**, *93*, 212. (b) Popelier, P. L. A. *Chem. Phys. Lett.* **1994**, *228*, 160.

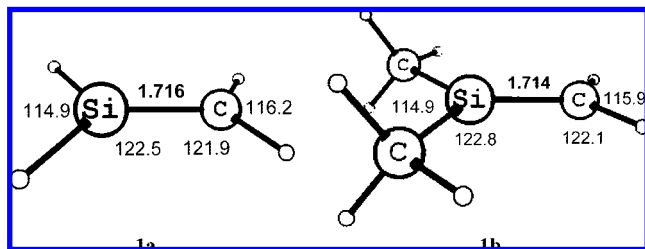
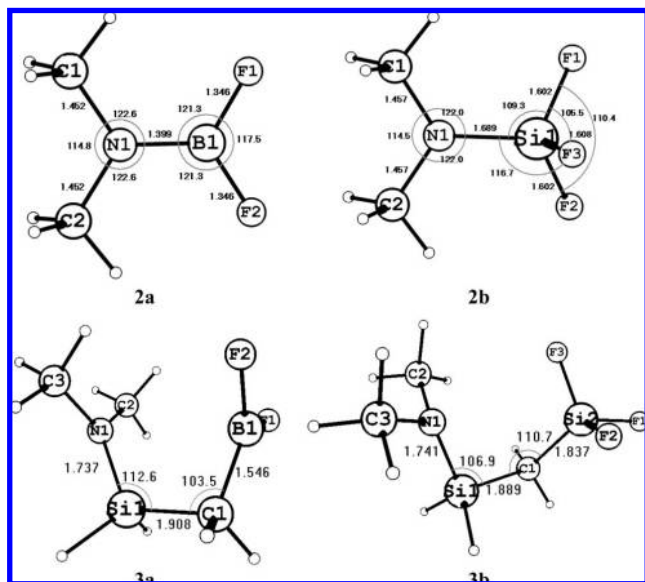
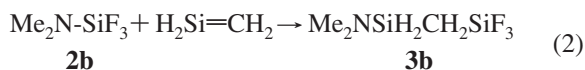
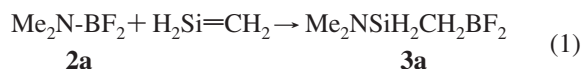


Figure 1. Optimized structures of silenes.

Figure 2. Optimized structures of ligands **2** and the insertion products **3**.

Although published previously,<sup>21</sup> we recalculated the structures of silene and 1,1-dimethylsilene (Figure 1), in order to properly compare them with silene moieties in our target complexes.

Attempted optimization of the desired silene complexes to (dimethylamino)difluoroborane, **2a**, and (dimethylamino)trifluorosilane, **2b** ( $n = 0$  ligands), resulted in the insertion products *gauche*-**3a** and *gauche*-**3b** of silene inserting into the N–B or N–Si bonds of the ligands.



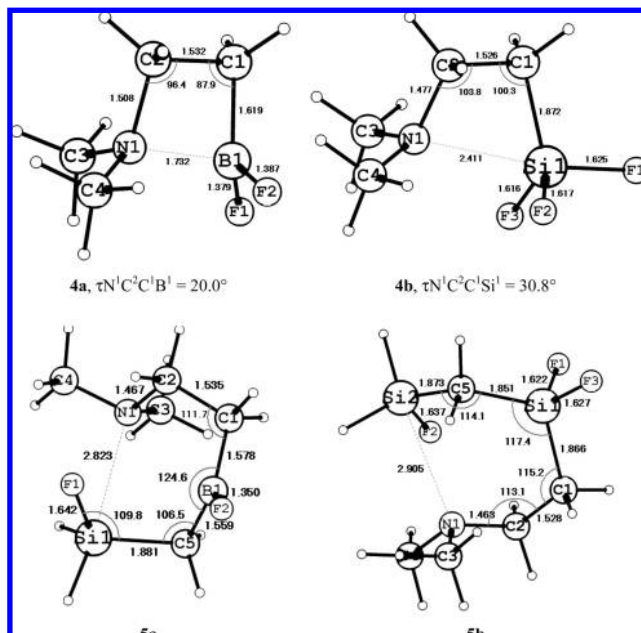
The optimized structures of the ligands and corresponding insertion products are shown in Figure 2, and the geometric parameters of **3a** and **3b** are given in Table 1.

The enthalpies of the insertion reaction to form **3a** and **3b** are  $-35.1$  and  $-49.3$  kcal/mol, respectively.

The data listed in Table 1 can be used for comparison with the geometric parameters of the ditopic complexes (see section 1.2). Of particular interest are the distances between nonbonded atoms  $\text{B} \cdots \text{N}$  in **3a** ( $2.995$  Å) and  $\text{Si} \cdots \text{N}$  in **3b** ( $3.258$  Å), which are shorter than the sums of van der Waals radii of the atoms themselves:  $r(\text{B}) + r(\text{N}) = 3.55$  Å;  $r(\text{Si}) + r(\text{N}) = 3.65$  Å.<sup>22</sup>

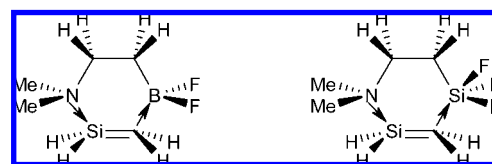
(21) Gusel'nikov, L. E.; Avakyan, V. G.; Guselnikov, S. L. *J. Am. Chem. Soc.* **2002**, *124*, 662.

(22) Bondi, A. J. *Phys. Chem.* **1964**, *68*, 441.

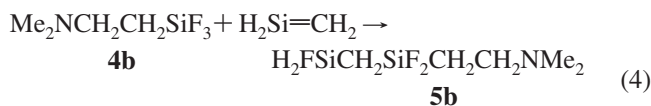
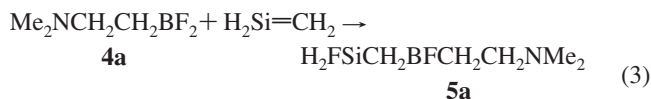
Figure 3. Optimized structures of ligands **4** and their insertion products **5**.Table 1. Relevant Geometric Parameters of the Insertion Products **3a** and **3b**

bond lengths (Å) and angles (deg)	<b>3a</b>	<b>3b</b>
$\text{B}^1\text{C}^1/\text{Si}^2\text{C}^1$	1.546/–	–/1.837
$\text{Si}^1\text{C}^1$	1.908	1.889
$\text{Si}^1\text{N}^1$	1.737	1.741
$\text{F}^1\text{B}^1$ , $\text{F}^2\text{B}^1/\text{F}^1\text{Si}^2$ , $\text{F}^2\text{Si}^2$ , $\text{F}^3\text{Si}^2$	1.341, 1.340/–	–/1.610, 1.608, 1.606
$\text{N}^1 \cdots \text{B}^1/\text{N}^1 \cdots \text{Si}^1$	2.995/–	–/3.258
$\text{F}^1\text{B}^1\text{C}^1\text{Si}^1$ , $\text{F}^2\text{B}^1\text{C}^1\text{Si}^1/\text{F}^1\text{Si}^2\text{C}^1\text{Si}^1$ , $\text{F}^2\text{Si}^2\text{C}^1\text{Si}^1$ , $\text{F}^3\text{Si}^2\text{C}^1\text{Si}^1$	–78.9, 96.6	–/–160.7, 42.1, –80.3,
$\text{B}^1\text{C}^1\text{Si}^1\text{N}^1/\text{Si}^2\text{C}^1\text{Si}^1\text{N}^1$	–21.4/–	–/40.1
$\text{C}^1\text{Si}^1\text{N}^1\text{C}^2$ , $\text{C}^1\text{Si}^1\text{N}^1\text{C}^3$	–73.3, 89.5	–65.0, 146.6

Scheme 3



*gauche*-(2-Dimethylaminoethyl)difluoroborane, **4a**, and *gauche*-(2-dimethylaminoethyl)trifluorosilane, **4b** ( $n = 2$  ligands), were probed for the six-membered cyclic silene complexes with two dative bonds, namely,  $\text{N} \rightarrow \text{Si}$ ,  $\text{C} \rightarrow \text{B}$  and  $\text{N} \rightarrow \text{Si}$ ,  $\text{C} \rightarrow \text{Si}$ , respectively (Scheme 3). However, these efforts resulted in the insertion products **5a** and **5b** of the silene into the B–F and Si–F bonds.

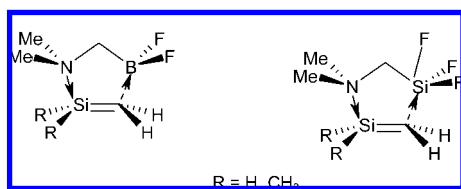


The optimized structures of the ligands and insertion products are shown in Figure 3.

The notable features of the ligands **4** are the very short distances between donor nitrogen and acceptor boron ( $1.732$  Å



Scheme 4



in **4a**) or silicon (2.411 Å in **4b**) atoms.<sup>23</sup> Presumably, the intramolecular N $\cdots$ B and N $\cdots$ Si interactions in **4a** and **4b** make ditopic complex formation unfavorable. Quasi-seven-membered cycles stabilized by a transannular N $\rightarrow$ Si interaction (2.823 and 2.904 Å) are inherent to the insertion products **5a** and **5b**.<sup>24</sup> Reaction enthalpies of the insertion product formation are  $-40.6$  and  $-49.5$  kcal/mol for **5a** and **5b**, respectively.

**1.2. Ditopic and  $n$ -Donor Silene Complexes to (Dimethylaminomethyl)difluoroborane and (Dimethylaminomethyl)trifluorosilane ( $n = 1$  ligands).** The structures of the ditopic silene complexes with methylene-bridged ligands could be expected to be the five-membered rings formed by two dative bonds: N $\rightarrow$ Si, C $\rightarrow$ B or N $\rightarrow$ Si, C $\rightarrow$ Si, respectively, as shown in Scheme 4.

There are two alternative pathways for forming ditopic complexes: via (i) the concerted coordination of the ligands to silenes or (ii) their consecutive coordination starting from the initial formation of N $\rightarrow$ Si or C $\rightarrow$ X (where X = B or Si) bonds. Both pathways were addressed.

**Geometries of Methylene-Bridged Ligands.** The optimized structures of (dimethylaminomethyl)difluoroborane (**6a**) and (dimethylaminomethyl)trifluorosilane (**6b**) are given in Figure 4.

We found conformer **6a** to be the most stable. In order to interact with the silenic carbon by concerted coordination, the BF<sub>2</sub> group in **6a** must be rotated to form the conformer **6a'**, in which the appropriate mutual orientation of the nitrogen's lone pair and boron's empty p-orbital is provided. Geometric parameters of the ditopic ligands are listed in Table 2.

Since the ligands contain both  $n$ -donor and acceptor groups joined to each other via the methylene bridge, it was suggested that the intramolecular donor–acceptor bonding (DAB) N $\rightarrow$ B in **6a'** and N $\rightarrow$ Si in **6b** would resist the concerted ditopic coordination to silenes. It seemed that the short contacts B $\cdots$ N (2.437 Å) in **6a'** and Si $\cdots$ N (2.748 Å) in **6b** should facilitate DAB. However, the study on the topology of the electron density distribution demonstrated no N $\rightarrow$ Si dative bond in F<sub>3</sub>SiCH<sub>2</sub>NMe<sub>2</sub>.<sup>25</sup> According to our AIM data we anticipated no DAB for **6a'** due to the absence of the bond critical point of rank (3,–1) at the boron and nitrogen internuclear area.

**Geometries of Ditopic and Related Silene Complexes to Methylene-Bridged Ligands.** The geometry optimizations of the expected ditopic silene complexes to **6a'** and **6b** resulted in structures **7** and **8** (Figure 5), for which the deep minima are inherent to the potential energy surface. Their geometric parameters are given in Table 3.

The concerted coordination of silenes **1** to the ligands **6** resulted in the cyclic five-membered semi-chair conformations of the complexes **7** and **8**, which were localized on PES substantially lower than the sum of energies of their precursors.

Components of the complexes are bonded by two dative bonds: N $\rightarrow$ Si and C $\rightarrow$ B (**7a** and **8a**), N $\rightarrow$ Si and C $\rightarrow$ Si (**7b** and **8b**) (Figure 5). Both the nitrogen and boron atoms occur in tetrahedral configuration, whereas silicon in the ligand moiety is pentacoordinated (Table 3). Besides, fluorine atoms occupy one axial and two equatorial positions in the trigonal bipyramid of C<sub>2</sub>SiF<sub>3</sub> coordination nodes in **7b** and **8b**. High degrees of tetrahedrality,  $\eta_t$ , are found for boron in **7a** (93%) and **8a** (95%). Similarly, the degree of trigonal pyramidalization, i.e., pentacoordination, of silicon,  $\eta_a$ , in **7b** (94%) and **8b** (97%) is extremely high and close to the ideal value of 100%.<sup>26</sup> Therefore, **7** and **8** are indeed ditopic donor–acceptor complexes.

The nonstrained structures of **7** and **8** are provided by the appropriate geometries of the ligands. We note the closeness of N $\cdots$ X contacts in free ligands and in the ligand moieties of the ditopic complexes, cf. B $\cdots$ N distances (Å) in **6a'** (2.437) with **7a** (2.558) and **8a** (2.561) and Si $\cdots$ N distances in **6b** (2.748) with **7b** (2.852) and **8b** (2.849).

The N $\rightarrow$ Si bonds in **7** (1.934 and 1.964 Å) and in **8** (1.943 and 1.943 Å) are shorter than those in silene's  $n$ -donor complexes (2.156–2.243 Å at MP2/6-31G\* level of theory<sup>6</sup>) but still 11.3–12.9% longer than the covalent N–Si bond in **3** (1.737–1.740 Å).<sup>27</sup> The dative C $\rightarrow$ B bonds in **7a** and **8a** (1.662 and 1.652 Å) are  $\sim 7\%$  longer than the covalent C–B bond in **3a** (1.547 Å). In turn, the dative C $\rightarrow$ Si bonds in **7b** and **8b** (2.015 and 1.910 Å) are 10% and 4% longer than the covalent C–Si bond in **3b** (1.833 Å). Furthermore, the complexation leads to the elongation of C–N and B–C/Si–C distances in the ligand fragment of the complexes with the respect to those in the free ligands.

The SiC bonds in **7a** and **8a** (1.827 and 1.834 Å) and **7b** and **8b** (1.812 and 1.849 Å) are substantially longer than in silene and dimethylsilene (1.716 and 1.714 Å), but shorter than the single Si–C bonds in **3a** (1.908 and 1.904 Å) and **3b** (1.889 and 1.891 Å), indicating a partial conservation of double bonding in the silenic moiety of the ditopic complexes. The latter conclusion is also confirmed when comparing the sums of the angles around Si- and C-nodes, reaching 343–349° and 331–334°, respectively. The degree of tetrahedrality of silenic carbon is far higher than that of the silicon in **7** and **8**: cf. 81% and 36% (**7a**); 85% and 35% (**7b**); 85% and 50% (**8a**); 81% and 54% (**8b**). Therefore, the carbon atom in the silenic moiety of **7** and **8** suffers the most significant geometry changes with respect to that in **1**. Of course, such drastic changes in geometry should result in the considerable loss of silene's  $\pi$ -electron density, which becomes partially involved in the dative bonding of silenic carbon to boron and silicon in **7** and **8**, respectively.

It is worth comparing the ditopic complexes **7** and **8** with  $n$ -donor ones, particularly because the latter could be the precursor of the former. Therefore  $n$ -donor complexes **9**–**11** of silenes with trimethylamine and the ligands **6a'** and **6b** were calculated (Figure 6, Table 4).

One can see that N $\rightarrow$ Si bonds in complexes **10** and **11** are somewhat elongated with respect to those in **9**, cf. 2.149 Å (**9a**) with 2.164 Å (**10a**) and 2.176 Å (**10b**); 2.231 Å (**9b**) with 2.250 Å (**11a**) and 2.268 Å (**11b**). Bond distances Si=C in **9**–**11** (1.719–1.722 Å) increase a little when compared with free silenes (1.716 Å in **1a** and 1.714 Å in **1b**), remaining substantially shorter than the ordinary Si–C bond (1.908 Å in

(23) (a) *gauche-4a* and *gauche-4b* ligands are 10–4.2 kcal/mol more stable than *trans-4a* and *trans-4b*, respectively.

(24) **5a** and **5b** are 3.7 and 4.8 kcal/mol more stable than their full *trans*-conformers.

(25) Mitzel, N. V.; Vojinovich, K.; Foerster, T.; Robertson, H.; Borisenko, K.; Rankin, D. W. H. *Chem. Eur. J.* **2005**, *11*, 5114.

(26) According to definition,  $\eta_a = (109.5 - 1/3 \sum_i^3 \angle Q_i) / (109.5 - 90) \times 100\%$ , where  $Q_i$  are the valence angles between axial and equatorial bonds;  $\eta_t = (120 - 1/3 \sum_i^3 \angle Q_i) / (120 - 109.5) \times 100\%$ , where  $Q_i$  are the valence angles for the C<sub>2</sub>BF<sub>2</sub> fragment; Tamao, K.; Hayashi, T.; Ito, Y.; Shiro, M. *Organometallics* **1992**, *11*, 2099.

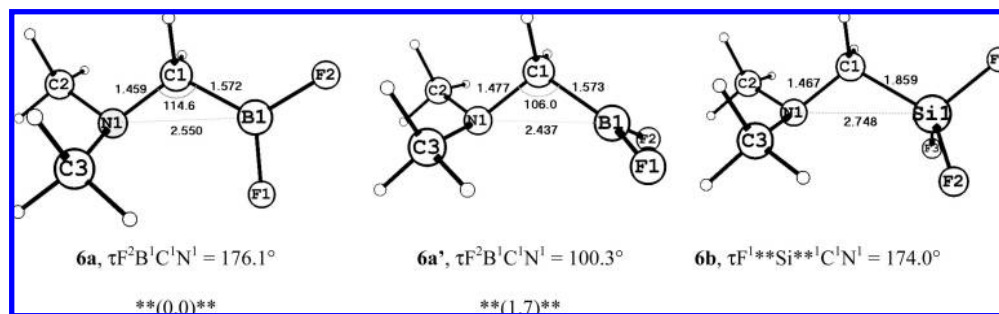


Figure 4. Optimized structures of ligands **6** and relative energies of **6a** and **6a'**, kcal/mol.

Table 2. Calculated Geometric Parameters of Methylene-Bridged Ligands

bond lengths (Å) and angles (deg)	<b>6a</b>	<b>6a'</b>	<b>6b<sup>a</sup></b>
B <sup>1</sup> C <sup>1</sup> /Si <sup>1</sup> C <sup>1</sup>	1.572/—	1.573/—	—/1.859 (1.854)
B <sup>1</sup> F <sup>1</sup> , B <sup>1</sup> F <sup>2</sup> /Si <sup>1</sup> F <sup>1</sup> , Si <sup>1</sup> F <sup>2</sup> , Si <sup>1</sup> F <sup>3</sup>	1.331, 1.336/—	1.333, 1.336/—	—/1.603, 1.607, 1.608 (1.567, 1.567, 1.567)
C <sup>1</sup> N <sup>1</sup>	1.459	1.477	1.467 (1.464)
N <sup>1</sup> C <sup>2</sup> , N <sup>1</sup> C <sup>3</sup>	1.457, 1.458	1.457, 1.459	1.460, 1.461 (1.456, 1.456)
B <sup>1</sup> ...N <sup>1</sup> /Si <sup>1</sup> ...N <sup>1</sup>	2.550/—	2.437/—	—/2.748 (2.731) <sup>b</sup>
C <sup>1</sup> N <sup>1</sup> C <sup>2</sup> , C <sup>1</sup> N <sup>1</sup> C <sup>3</sup>	110.4, 110.7	107.9, 110.6	110.7, 110.7 (111.5, 111.5)
C <sup>2</sup> NC <sup>3</sup>	109.9	109.8	109.9 (107.3)
B <sup>1</sup> C <sup>1</sup> N <sup>1</sup> /Si <sup>1</sup> C <sup>1</sup> N <sup>1</sup>	114.7/—	106.0/—	—/110.9 (110.3)
F <sup>1</sup> B <sup>1</sup> C <sup>1</sup> , F <sup>2</sup> B <sup>1</sup> C <sup>1</sup> /F <sup>1</sup> Si <sup>1</sup> C <sup>1</sup> , F <sup>2</sup> Si <sup>1</sup> C <sup>1</sup> , F <sup>3</sup> Si <sup>1</sup> C <sup>1</sup>	119.6, 123.7/—	121.4, 122.2/—	—/109.8, 111.0, 114.2 (111.2, 112.0, 112.6)
F <sup>1</sup> B <sup>1</sup> F <sup>2</sup> /F <sup>1</sup> Si <sup>1</sup> F <sup>2</sup> , F <sup>1</sup> Si <sup>1</sup> F <sup>3</sup> , F <sup>2</sup> Si <sup>1</sup> F <sup>3</sup>	116.7/—	116.7/—	—/106.9, 107.3, 107.4,
F <sup>1</sup> ²B <sup>1</sup> C <sup>1</sup> N <sup>1</sup> , F <sup>2</sup> ²B <sup>1</sup> C <sup>1</sup> N <sup>1</sup> /F <sup>1</sup> Si <sup>1</sup> C <sup>1</sup> N <sup>1</sup> , F <sup>2</sup> Si <sup>1</sup> C <sup>1</sup> N <sup>1</sup> , F <sup>3</sup> Si <sup>1</sup> C <sup>1</sup> N <sup>1</sup>	—6.0, 175.4/—	—77.2, 100.3/—	—/53.9, —67.5, 174.0 (177.9)
B <sup>1</sup> C <sup>1</sup> N <sup>1</sup> C <sup>2</sup> , B <sup>1</sup> C <sup>1</sup> N <sup>1</sup> C <sup>3</sup> , Si <sup>1</sup> C <sup>1</sup> N <sup>1</sup> C <sup>2</sup> , Si <sup>1</sup> C <sup>1</sup> N <sup>1</sup> C <sup>3</sup>	—68.7, 168.4/—	—157.4, 80.6/—	—/81.7, —156.1 (90.9, —149.1)

<sup>a</sup> Gas electron diffraction data<sup>25</sup> are given in parentheses. <sup>b</sup> Si<sup>1</sup>...N<sup>1</sup> distance was evaluated using Cartesian coordinates taken from Supporting Information given in ref 25.

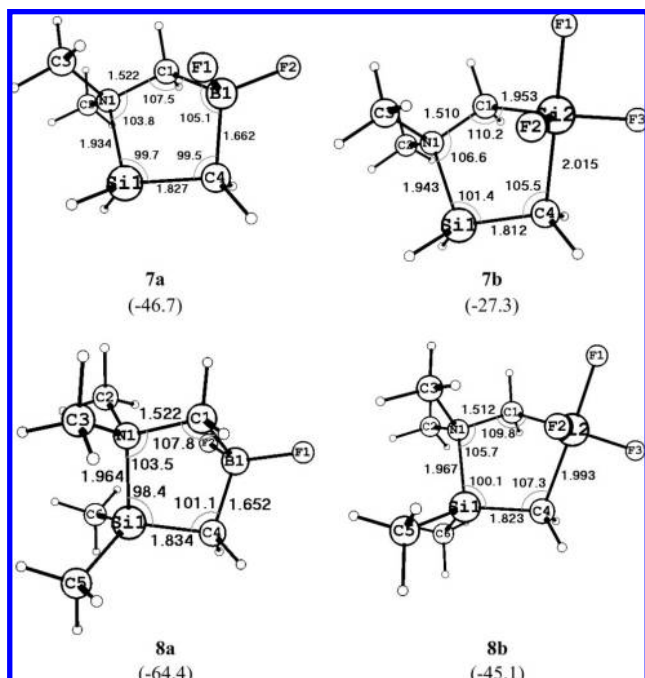


Figure 5. Optimized structures of the ditopic silene and dimethylsilene complexes to methylene-bridged ligands **7** and **8** and their complexation energies, kcal/mol.

**3a** and 1.889 Å in **3b**). The degree of tetrahedrity of the silenic carbon in *n*-donor complexes is close to 0% (cf. >80% for **7** and **8**), whereas for the silicon atom it is approximately half as much (20% in **10a**; 18% in **10b**; 26% in **11a**; 23% in **11b**) as that in **7** and **8** (35–54%).

We also checked whether complexation of silenes could occur via the only C→X (where X = B or Si) dative bonding. The attempted modeling of H<sub>2</sub>Si=CH<sub>2</sub>→BF<sub>2</sub>CH<sub>2</sub>NMe<sub>2</sub> and Me<sub>2</sub>Si=CH<sub>2</sub>→BF<sub>2</sub>CH<sub>2</sub>NMe<sub>2</sub> complexes resulted however in adducts formed by the insertion of silene into the B–F bond, i.e. *trans*-H<sub>2</sub>FSiCH<sub>2</sub>BFCH<sub>2</sub>NMe<sub>2</sub> (**12a**) and *trans*-Me<sub>2</sub>FSiCH<sub>2</sub>BFCH<sub>2</sub>NMe<sub>2</sub> (**13a**), whose optimized structures are shown in Figure 7.

Optimization of the complex formed by only a C→Si dative bond, H<sub>2</sub>Si=CH<sub>2</sub>→SiF<sub>3</sub>CH<sub>2</sub>NMe<sub>2</sub>, resulted in a weak van der Waals complex (**14**) (Figure 7).

**Energetics.** The complexation energies for the interaction of silenes **1** with ligands **6** and enthalpies of silenes' insertion into the ligand **6a'** are listed in Table 5.

The concerted reaction of parent silene and dimethylsilene to methylene-bridged ligands **6a'** and **6b** resulted in complexation energies reaching –64.4 kcal/mol, being more exothermic for boron-containing ligands by approximately 19 kcal/mol, cf. differences: 19.4 kcal/mol (between **7a** and **7b**) and 19.3 kcal/mol (between **8a** and **8b**). The strong acceptor ability of **6a'** is due to an empty orbital on boron, while the propensity for hypercoordination is a driving force for somewhat weaker dative bonding to the electronically saturated silicon atom in **6b**. Also, due to the stronger electrophilicity of silicon surrounded by methyl substituents, ditopic complexes of dimethylsilene are approximately 18 kcal/mol more stable than those of silene, cf. differences: 17.7 kcal/mol (between **8a** and **7a**) and 17.8 kcal/mol (between **8b** and **7b**).

Complexation of the silenes to **6a'** via the only N→Si dative bond BF<sub>2</sub>CH<sub>2</sub>NMe<sub>2</sub>→H<sub>2</sub>Si=CH<sub>2</sub> and SiF<sub>3</sub>CH<sub>2</sub>NMe<sub>2</sub>→H<sub>2</sub>Si=CH<sub>2</sub> resulted in *n*-donor complexes **10a** and **10b** that are 40.4 and 20.1 kcal/mol less stable than the corresponding ditopic complexes **7a** and **7b**. More stable *n*-donor complexes

Table 3. Calculated Geometric Parameters of Ditopic Complexes

bond lengths (Å) and angles (deg)	7a	7b	8a	8b
N <sup>1</sup> —Si <sup>1</sup>	1.934	1.943	1.964	1.967
Si <sup>1</sup> =C <sup>4</sup>	1.827	1.812	1.834	1.823
C <sup>4</sup> —B <sup>1</sup> /C <sup>4</sup> —Si <sup>2</sup>	1.662/—	—/2.015	1.652/—	—/1.993
B <sup>1</sup> —C <sup>1</sup> /Si <sup>2</sup> —C <sup>1</sup>	1.646/—	—/1.953	1.646/—	—/1.956
C <sup>1</sup> —N <sup>1</sup>	1.522	1.510	1.522	1.512
B <sup>1</sup> ...N <sup>1</sup> /Si <sup>1</sup> ...N <sup>1</sup>	2.558/—	—/2.852	2.561/—	—/2.897
N <sup>1</sup> —C <sup>2</sup> , N <sup>1</sup> —C <sup>3</sup>	1.486, 1.494	1.487, 1.496	1.485, 1.493	1.496, 1.487
Si <sup>1</sup> —H <sup>a</sup> /Si—C <sup>5</sup> , Si—C <sup>6</sup>	1.475, 1.482/—	1.474, 1.481/—	—/1.876, 1.883	—/1.875, 1.883
B <sup>1</sup> —F <sup>1</sup> , B <sup>1</sup> —F <sup>2</sup> /Si—F <sup>1</sup> , Si—F <sup>2</sup> , Si—F <sup>3</sup> , N <sup>1</sup> Si <sup>1</sup> C <sup>4</sup>	1.398, 1.442/—	—/1.671, 1.664, 1.644,	1.401, 1.447/—	—/1.671, 1.646, 1.675
Si <sup>1</sup> C <sup>4</sup> B <sup>1</sup> /Si <sup>1</sup> C <sup>4</sup> Si <sup>2</sup>	99.7	101.4	98.4	100.1
C <sup>4</sup> B <sup>1</sup> C <sup>1</sup> /C <sup>4</sup> Si <sup>2</sup> C <sup>1</sup>	99.5/—	—/105.5	101.1/—	—/107.3
B <sup>1</sup> C <sup>1</sup> N <sup>1</sup> /Si <sup>2</sup> C <sup>1</sup> N <sup>1</sup>	105.3/—	—/88.6	104.7/—	—/88.0
C <sup>1</sup> N <sup>1</sup> Si <sup>1</sup>	107.5/—	—/110.2	107.8/—	—/109.8
C <sup>4</sup> B <sup>1</sup> F <sup>1</sup> , C <sup>4</sup> B <sup>1</sup> F <sup>1</sup> /C <sup>4</sup> Si <sup>2</sup> F <sup>1</sup> , C <sup>4</sup> Si <sup>2</sup> F <sup>2</sup> , C <sup>4</sup> Si <sup>2</sup> F <sup>3</sup>	103.8	106.6	103.5	105.7
F <sup>1</sup> B <sup>1</sup> F <sup>2</sup> /F <sup>1</sup> SiF <sup>2</sup> , F <sup>1</sup> SiF <sup>3</sup> , F <sup>2</sup> SiF <sup>3</sup>	106.8, 113.8/—	—/179.0, 88.9, 89.0,	114.4, 107.3/—	—/89.1, 90.2, 178.0
C <sup>1</sup> N <sup>1</sup> C <sup>2</sup> , C <sup>1</sup> N <sup>1</sup> C <sup>3</sup>	111.2/—	—/91.8, 91.4, 122.3	110.8/—	—/91.1, 91.3, 122.2
C <sup>2</sup> N <sup>1</sup> C <sup>3</sup>	108.6, 109.3,	108.5, 108.7,	107.8, 108.6,	107.6, 108.1,
C <sup>2</sup> N <sup>1</sup> Si <sup>1</sup> , C <sup>2</sup> N <sup>1</sup> Si <sup>1</sup>	111.7	111.0	111.1	110.6
HSi <sup>1</sup> C <sup>4b</sup> /C <sup>5</sup> Si <sup>1</sup> C <sup>4</sup> , C <sup>6</sup> Si <sup>1</sup> C <sup>4</sup>	110.9, 112.4	110.3, 111.7	113.8, 112.0	111.5, 113.2
HSi <sup>1</sup> H/C <sup>5</sup> SiC <sup>5</sup>	118.6, 121.2/—	119.0, 120.9/—	—/116.1, 118.5	—/116.9, 117.2
sum of angles around Si-node	108.7/—	—/109.0	109.6/—	—/110.1
HC <sup>4</sup> Si <sup>1c</sup>	348.5	348.9	344.2	344.2
HC <sup>4</sup> H	113.0, 112.1	112.6, 111.8	112.0, 112.3	111.0, 111.8,
sum of angles around C-node	109.3,	108.9	108.8	108.5
N <sup>1</sup> Si <sup>1</sup> C <sup>4</sup> B <sup>1</sup> /N <sup>1</sup> Si <sup>1</sup> C <sup>4</sup> Si <sup>2</sup>	334.4	333.3	333.1	331.3
Si <sup>1</sup> C <sup>4</sup> B <sup>1</sup> C <sup>1</sup> /Si <sup>1</sup> C <sup>4</sup> Si <sup>2</sup> C <sup>1</sup>	24.6/—	—/24.0	23.1/—	—/21.2
C <sup>4</sup> B <sup>1</sup> C <sup>1</sup> N <sup>1</sup> /C <sup>4</sup> Si <sup>2</sup> C <sup>1</sup> N <sup>1</sup>	—44.7/—	—/—41.5	—44.5/—	—/—40.4
B <sup>1</sup> C <sup>1</sup> N <sup>1</sup> Si <sup>1</sup> /Si <sup>2</sup> C <sup>1</sup> N <sup>1</sup> Si <sup>1</sup>	52.1/—	—/52.7	52.9/—	—/54.3
C <sup>1</sup> N <sup>1</sup> Si <sup>1</sup> C <sup>4</sup>	—31.5/—	—/—42.5	—33.3/—	—/—46.0
	3.7	9.9	5.6	14.1

<sup>a</sup> Two values for Si<sup>1</sup>—H bond distances in the silene moiety. <sup>b</sup> Two values for HSi<sup>1</sup>C<sup>4</sup> angles in the silene moiety. <sup>c</sup> Two values for HC<sup>4</sup>Si<sup>1</sup> angles in the silene moiety.

**11a** and **11b**, BF<sub>2</sub>CH<sub>2</sub>NMe<sub>2</sub>→Me<sub>2</sub>Si=CH<sub>2</sub> and SiF<sub>3</sub>CH<sub>2</sub>NMe<sub>2</sub>→Me<sub>2</sub>Si=CH<sub>2</sub>, are obtained via the complexation of **6a'** and **6b** to dimethylsilene. Both were less stable than the ditopic complexes **8a** and **8b** by 44.4 and 23.7 kcal/mol, respectively. The insertion products of silenes into the B—F bond of **6a'**, i.e., *trans*-H<sub>2</sub>FSiCH<sub>2</sub>BFCH<sub>2</sub>NMe<sub>2</sub> (**12a**), appeared to be 2.2 kcal/mol less stable than **7a**, whereas *trans*-Me<sub>2</sub>FSiCH<sub>2</sub>BFCH<sub>2</sub>NMe<sub>2</sub> (**13a**) was 1.4 kcal/mol more stable than **8a**. Therefore, ditopic complexation of silene to **6a'** should not be suppressed by the competitive insertion into its B—F bond, but this might be not so in the case of dimethylsilene. Nevertheless, irrespective of relative energies of the complexation and insertion reactions, no rearrangements of ditopic complexes and insertion products were observed upon the optimizations.

We also optimized dimers of **6a'** and **6b** (whose geometries are given in the Supporting Information) and determined dimerization energies equal to −56.7 and −4.5 kcal/mol, respectively. When comparing the latter quantities to the complexation energies (see Table 5), one may deduce that dimerization can compete with ditopic coordination to the parent silene only for boranyl ligand **6a'**. However, no competition is expected for dimethylsilene, **1b**, because the ditopic coordination of **6a'** to **1b** is 7.7 kcal/mol more preferable than the dimerization. The ditopic coordination of silyl ligand **6b** to silene and dimethylsilene is far more exothermic (by 22.8 and 40.6 kcal/mol, respectively) than the enthalpy of **6b** dimerization. Ditopic ligand—silene complexation is also feasible not only from the computational prediction but also from experimental observation of no **6b** dimerization in the gas phase.<sup>25</sup> Attempted

optimization of the complex formed with only a C→Si dative bond resulted in the formation of the weak van der Waals complex **14**, which was 25.2 kcal/mol less stable than **7b**. Therefore, one can expect that ditopic complexes **7b** and **8b** will be the most likely products of the ditopic coordination of dimethylsilene **1b** to the ligand **6b**.

Comparing Δ*E* values calculated at 0 K with Δ*G*<sup>298.15</sup> ones, it is seen that temperature increase makes the complexation energies less exothermic and even endothermic in the case of *n*-donor and van der Waals complexes. However, for higher temperature the formation of ditopic complexes **7b** and **8b** still remains the most preferable process, whereas both **7a** and **8a** formations become noncompetitive with the insertion reactions, leading to **12a** and **13a**, respectively.

**AIM Analysis.** The evidence for dative N→Si, C→Si, and C→B binding in **7–11** emerging from the above structural and energetic data is confirmed by the discovery of the bond critical point (BCP) of rank (3, −1) in the internuclear area between donor and acceptor atoms of the all complexes studied. The presence of the ring critical point of rank (3, +1) located approximately in the center of NSiCBC and NSiCSiC skeletons is indicative of the cyclic structure of the ditopic complexes, as shown in Figure 8 in the case of a molecular graph describing **8b**.

The topological indices of the Si—C, Si=C, N→Si, C→B, and C→Si bonds are given in Table 6.

The electron density of dative C→B bonds in **7a** and **8a** (0.978–1.002 e/Å<sup>3</sup>) is somewhat lower than that of the ordinary



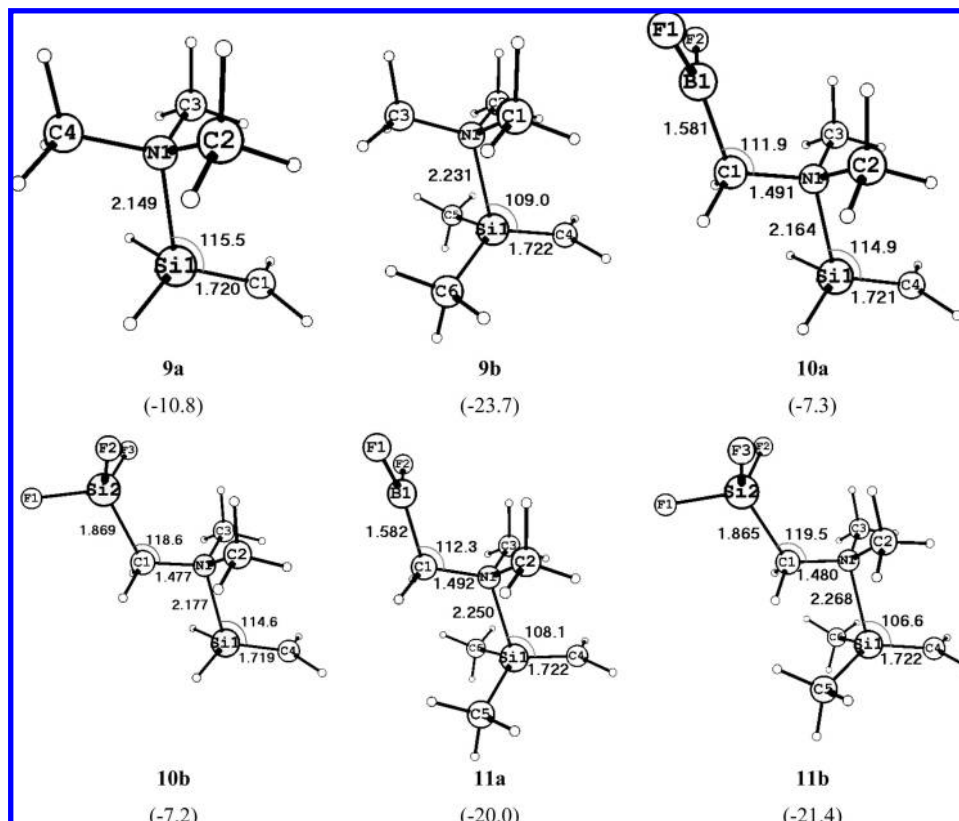


**Figure 6.** Optimized structures of *n*-donor silene complexes to trimethylamine and ditopic ligands **9–11** and their complexation energies, kcal/mol.

**Table 4.** Relevant Geometric Parameters of *n*-Donor Complexes

bond lengths (Å) and angles (deg)	<b>9a</b>	<b>9b</b>	<b>10a</b>	<b>10b</b>	<b>11a</b>	<b>11b</b>
N <sup>1</sup> →Si <sup>1</sup>	2.149	2.231	2.164	2.176	2.250	2.268
Si <sup>1</sup> =C <sup>4</sup>	1.720	1.722	1.721	1.719	1.722	1.722
C <sup>1</sup> –B <sup>1</sup> /C <sup>1</sup> –Si <sup>2</sup>			1.581/–	–/1.869	1.582/–	–/1.865
C <sup>1</sup> –N <sup>1</sup>			1.491	1.477	1.492	1.480
C <sup>4</sup> Si <sup>1</sup> N <sup>1</sup>	115.4	119.5	114.8	114.6	108.1	106.6
Si <sup>1</sup> N <sup>1</sup> C <sup>1</sup> , Si <sup>1</sup> N <sup>1</sup> C <sup>2</sup> , Si <sup>1</sup> N <sup>1</sup> C <sup>3</sup>	107.3, 107.3, 110.6	117.8, 105.0, 105.0				
Si <sup>1</sup> N <sup>1</sup> C <sup>2</sup> , Si <sup>1</sup> N <sup>1</sup> C <sup>3</sup>			106.7, 106.7	106.4, 106.4	104.4, 104.4	102.7, 104.1
Si <sup>1</sup> N <sup>1</sup> C <sup>1</sup>			109.4	108.6	116.6	102.7
HC <sup>4</sup> Si <sup>1a</sup>	121.9, 121.9	122.2, 122.2	122.0, 122.0	122.2, 122.2	121.9, 121.9	122.1, 122.2
HC <sup>4</sup> H	116.1	115.7	115.9	117.1	116.2	115.7
sum of angles around C-node	359.9	360.1	359.9	361.5	360	360
C <sup>4</sup> Si <sup>1</sup> H <sup>b</sup> /C <sup>4</sup> Si <sup>1</sup> C <sup>5</sup> , C <sup>4</sup> Si <sup>1</sup> C <sup>6</sup>	120.6, 120.6/–	–/119.5, 119.5	120.6, 120.7/–	–/119.6, 119.6	121.1, 121.1/–	–/120.0, 120.4
HSi <sup>1</sup> H/C <sup>5</sup> Si <sup>1</sup> C <sup>6</sup>	112.2/–	–/112.2	112.4/–	–/112.7	–/112.2	–/112.2
sum of angles around Si-node	353.4	351.2	353.7	351.9	354.4	352.6
C <sup>4</sup> Si <sup>1</sup> N <sup>1</sup> C <sup>2</sup> , C <sup>4</sup> Si <sup>1</sup> N <sup>1</sup> C <sup>3</sup>	59.0, –59.0	57.4, –57.2	58.7, –58.8	58.7, –58.7	57.4, –57.2	–71.2, –175.8
C <sup>4</sup> Si <sup>1</sup> N <sup>1</sup> C <sup>1</sup>	180.0	180.0,	180.0	180.0	180.0,	71.2
Si <sup>1</sup> N <sup>1</sup> C <sup>1</sup> B <sup>1</sup> / Si <sup>1</sup> N <sup>1</sup> C <sup>1</sup> Si <sup>2</sup>			180.0/–	–/180.0	180.0/–	–/166.7
N <sup>1</sup> C <sup>1</sup> B <sup>1</sup> F <sup>1</sup> , N <sup>1</sup> C <sup>1</sup> B <sup>1</sup> F <sup>2</sup> /N <sup>1</sup> C <sup>1</sup> Si <sup>2</sup> F <sup>1</sup> , N <sup>1</sup> C <sup>1</sup> Si <sup>2</sup> F <sup>2</sup> , N <sup>1</sup> C <sup>1</sup> Si <sup>2</sup> F <sup>3</sup>			88.4, –88.5/–	–/60.5, –60.7, 179.9	88.8, –88.8/–	–/54.7, –66.9, 173.6

<sup>a</sup> Two values for HC<sup>4</sup>Si<sup>1</sup> angles in the silene moiety. <sup>b</sup> Two values for C<sup>4</sup>Si<sup>1</sup>H angles in the silene moiety.

C–B bond in **3a** (1.285 e/Å<sup>3</sup>).<sup>22</sup> A similar, but more pronounced trend is observed for dative C→Si and ordinary C–Si bonds (cf. 0.624 and 0.746 in **7b** and **8b** with 0.886 e/Å<sup>3</sup> in **3b**). The lower electron density at the BCP of dative N→Si bonds is

characteristic of *n*-donor and ditopic complexes with respect to the ordinary N–Si bond in **3** (cf. 0.385 and 0.342 e/Å<sup>3</sup> in **9a** and **9b**; 0.589 and 0.574 e/Å<sup>3</sup> in **7a** and **8a**; 0.847 e/Å<sup>3</sup> in **3a**

(27) A comparison with **3a** and **3b** is appropriate because of the same surroundings about the skeletons: N–Si–C–B and N→Si–C→B, N–Si–C–Si and N→Si–C→Si.

(28) (a) Cremer, D.; Kraka, E. *Croat. Chem. Acta*. **1984**, 57, 1259. (b) Cremer, D.; Kraka, E. *Angew. Chem.* **1984**, 96, 612. (c) Cremer, D.; Kraka, E. *Angew. Chem., Int. Ed. Engl.* **1984**, 23, 627. (d) Ritchie, J. P.; Bachrach, S. M. *J. Am. Chem. Soc.* **1987**, 109, 5909.

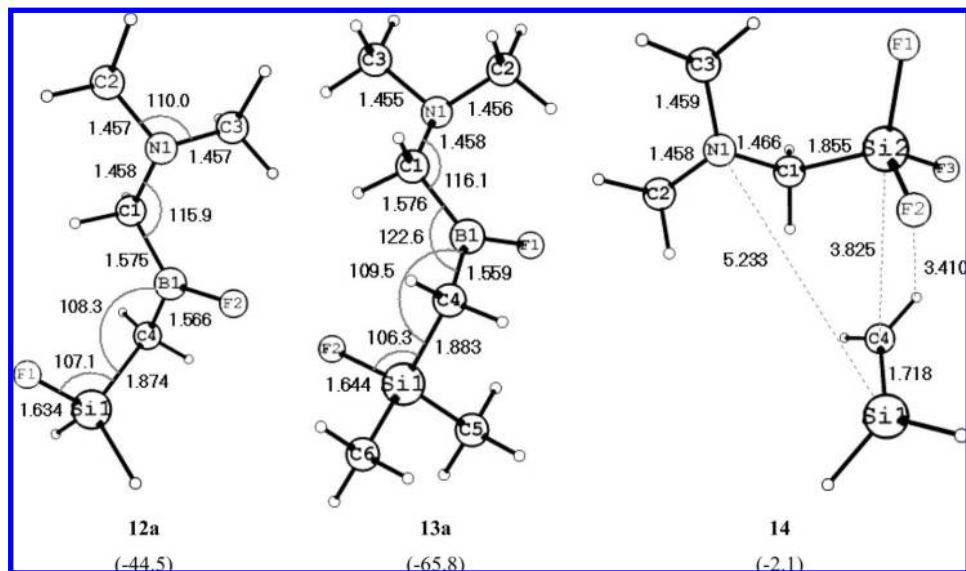


**Figure 7.** Optimized structures of the insertion products **12a** and **13a** and van der Waals complex **14** and their insertion and complexation energies, kcal/mol.

**Table 5.** Complexation Energy, kcal/mol

complex or adduct	$\Delta E$	$\Delta G^{298.15}$
<b>7a</b>	-46.7	-34.1
<b>7b</b>	-27.3	-13.6
<b>8a</b>	-64.4	-36.1
<b>8b</b>	-45.1	-15.3
<b>9a</b>	-10.8	0.5
<b>9b</b>	-23.7	3.1
<b>10a</b>	-7.3	2.7
<b>10b</b>	-7.2	4.1
<b>11a</b>	-20.0	5.2
<b>11b</b>	-21.4	5.2
<b>12a</b>	-44.5 <sup>a</sup>	-35.2 <sup>a</sup>
<b>13a</b>	-65.8 <sup>b</sup>	-40.4 <sup>b</sup>
<b>14</b>	-2.1	6.1

<sup>a</sup> Energy of silene insertion into the B-F bond of ligand **6a'**.

<sup>b</sup> Energy of dimethylsilene insertion into the B-F bond of ligand **6a'**.

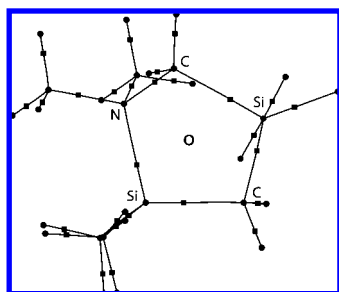


**Figure 8.** Molecular graph of ditopic dimethylsilene complex to (dimethylaminomethyl)trifluorosilane (bond critical points are shown by dark squares; a ring critical point is denoted by the circle).

and **3b**). Note that the electron density,  $\rho$ , at the BCP in ditopic complexes is greater than in *n*-donor ones. Lastly, all the electron densities inversely correlate well with the ordinary, dative, and double-bond distances (Figure 9).

Of special interest are the values of  $\rho$  at the BCP of the silenic moiety, being between that of the Si=C double bond in silenes **1** and ordinary Si<sup>1</sup>-C<sup>1</sup> bonds in **3**. These unambiguously indicate the partial doubly bonded character of the silenic moiety in ditopic complexes.

C→B bonds in **7a** and **8a** are, by the Cremer and Kraka criterion,<sup>28</sup> covalent ( $\nabla^2\rho < 0$ ;  $E_e < 0$ ), whereas C→Si and

N→Si are intermediate between ionic ( $\nabla^2\rho > 0$ ) and covalent ( $E_e < 0$ ), i.e. weak polar covalent bond (see Table 5). The latter is true for N→Si in *n*-donor complexes **9**–**11** despite the longer distance (2.149–2.268 Å) and lower electron density at the BCP (Table 5). The Si=C bonds in **1** and **7**–**11** rise in polarity in the order **1** < **9**–**11** < **7**, **8**. This is illustrated by AIM charges on Si and C atoms in the silene moiety (Figure 10).

Noteworthy is that the negative charge on nitrogen also increases on going from *n*-donor to ditopic complexes (cf. **10a** and **7b** in Figure 10).

The changes in the electron charge distribution for dimethylsilene and its *n*-donor and ditopic complexes are visually traced on Laplacian maps shown in Figure 11.

It is seen that nitrogen lone pairs responsible for N→Si bond formation in *n*-donor complexes **9b**–**11b** are polarized in the direction of the silicon atom. However, BCP remains out of the charge concentration area. In ditopic complexes the polarization is even greater, and the charge concentration area reaches BCP.  $\pi$ -Electron density distribution for the Si=C moieties of **1b** and **9b**–**11b** is visualized by two “tongues” of an electron cloud that does not belong to atomic basin of carbon and wraps a silicon from the top and bottom. On the contrary, in **8a** and **8b** charge is concentrated in the basin of silenic carbon and the electron cloud is highly polarized in the direction of acceptor boron or silicon atoms, respectively. Therefore, one may conclude that both dative C→B and C→Si bonds are formed by accepting a considerable portion of silene  $\pi$ -electron density by boron and silicon, respectively.

AIM analysis cannot reveal the multiplicity of a bond, but indirectly it may be estimated via ellipticity,  $\epsilon$ , and electron density at the BCP (see Table 5). Indeed,  $\epsilon$  spans from nonzero values for the double bond to practically zero ones for ordinary and triple bonds, whereas  $\rho$  increases in the order  $\rho(A-B) < \rho(A=B) < \rho(A\equiv B)$ .<sup>16a,b</sup> In our case,  $\epsilon$  is close to 0.5 for both silenes and *n*-donor complexes, but it drastically falls in ditopic complexes to 0.08 (**7a**), 0.1 (**7b**), and 0.07 (**8**). The rather low values of  $\epsilon$  for ditopic complexes still remain substantially higher than  $\epsilon$  for ordinary SiC bonds in **3a** and **3b** (0.02).

Table 6. Properties of the Bond Critical Points in **1**, *trans*-**3**, and **7–11**<sup>a</sup>

molecules and complexes	Si–C or Si=C				N–Si or N→Si			C→X (X = B, Si)		
	$\rho(r)$	$\nabla^2\rho(r)$	$\varepsilon$	$E_c(r)$	$\rho(r)$	$\nabla^2\rho(r)$	$E_c(r)$	$\rho(r)$	$\nabla^2\rho(r)$	$E_c(r)$
<b>1a</b>	0.963	13.115	0.51	−0.57						
<b>1b</b>	0.967	13.177	0.54	−0.57						
<b>3a</b>	0.736	5.157	0.02		0.844	14.941		1.862	−22.581	
<b>3b</b>	0.759	6.061	0.02		0.846	14.638		0.884	6.560	
<b>7a</b>	0.878	6.471	0.08	−0.58	0.589	6.512	−0.26	0.978	−1.767	−0.94
<b>7b</b>	0.891	7.208	0.10	−0.58	0.574	6.324	−0.25	0.624	3.414	−0.38
<b>8a</b>	0.875	6.522	0.07	−0.58	0.558	5.622	−0.25	1.002	−1.972	−0.97
<b>8b</b>	0.844	6.214	0.07	−0.55	0.580	6.367	−0.25	0.746	5.628	−0.46
<b>9a</b>	0.963	12.241	0.46	−0.58	0.385	2.033	−0.16			
<b>9b</b>	0.964	12.197	0.46	−0.59	0.342	0.883	−0.15			
<b>10a</b>	0.961	12.225	0.47	−0.58	0.378	1.73	−0.16			
<b>10b</b>	0.965	12.356	0.47	−0.58	0.371	1.602	−0.16			
<b>11a</b>	0.964	12.239	0.47	−0.59	0.336	0.664	−0.14			
<b>11b</b>	0.964	12.233	0.47	−0.59	0.327	0.552	−0.14			

<sup>a</sup>  $\rho(r)$ , charge density at the BCP in  $e/\text{\AA}^3$ ;  $\nabla^2\rho(r)$ , Laplacian of  $\rho(r)$  at the BCP in  $e/\text{\AA}^5$ ;  $\varepsilon$ , ellipticity;  $E_c(r)$ , local energy density in Hartree/ $\text{\AA}^3$ .

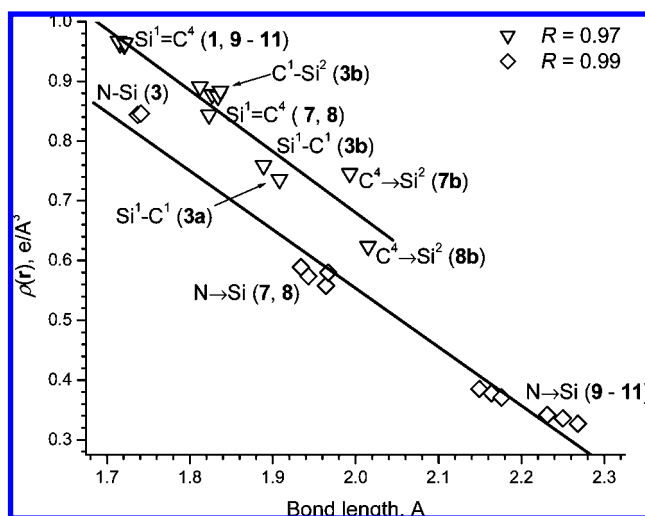


Figure 9. Plots of BCP electron densities vs bond lengths for bonds of silicon to nitrogen and carbon.

**ELF Analysis.** Disynaptic shape of valence basins (Figure 12) and their mean population<sup>29</sup> close to 2 (Table 7) indicate a covalent nature of the dative N→Si, C→Si, and C→B bonds in ditopic complexes **7** and **8**.

In accordance with ELF topology, the multiple bonds are manifested as two clearly distinct disynaptic basins with two weakly separated maxima above and below the Si–C axis and a local minimum on the Si–C vector.<sup>30</sup> Indeed, such shape of the disynaptic basins between silicon and carbon cores V1(Si¹,C) and V2(Si¹,C) and total population  $N \sim 3.7$  that is close to 4 attest to the Si=C bonds in **1** and **9–11** possessing pronounced  $\pi$ -character. However, in contrast to **1**, the bent disynaptic basin of the double bonds in **9–11** is directed to the carbon atom. This is due to the repulsive interaction of the electron clouds of Si=C and N→Si bonds, which leads to the inequivalence of V1 and V2 basins of the double bond (see Table 6). There is only one valence disynaptic basin in the interatomic area between silicon and carbon in the silene moiety of ditopic complexes **7** and **8**, whose volume and mean population (46.89–38.56 and 2.12–2.01, respectively) are rather similar to an ordinary SiC bond (see Appendix).

Concerning the two-step mechanism of the ditopic complexes formation, both AIM analysis (the polarity increase of the Si=C

bond due to the  $n$ -donor complexation, Figure 10) and ELF topology (the flexure of the Si=C electron cloud in the direction of the silenic carbon atom, Figure 12, **9a**) point at the preliminary N→Si coordination bond formation to impart silenic carbon donor properties, which prompt ditopic complex formation.

## Conclusion

Seeking bidentate ligands capable of forming ditopic self-assembly complexes with silenes,  $R_2Si=CH_2$ , we selected two types of candidates,  $Me_2N(CH_2)_nX$  ( $n = 0–2$ ;  $X = BF_2, SiF_3$ ). These ligands, containing both donor and acceptor sites, were expected to donate the nitrogen lone pair to  $sp^2$ -hybridized silicon and to accept the extra negative charge from the silenic carbon by boron (strong acceptor) or silicon (moderate acceptor) atoms of the Si=C moiety. The ab initio study at the MP4/6-311G(d,p)/MP2/6-31G(d,p)+ZPE level of theory of the concerted complexation of the parent silene ( $R = H$ ) and dimethylsilene ( $R = Me$ ) to methylene-bridged ligands **6a'** and **6b** ( $n = 1$ ) resulted in successful optimization of the ditopic silene complexes **7** and **8** formed by both N→Si and novel dative bonds of silenic carbon to boron (C→B) or silicon (C→Si), whose complexation energies reached −64.4 kcal/mol, being higher for boryl ligand by approximately 19 kcal/mol. The strong acceptor ability of **6a'** is due to an empty orbital on boron, while the propensity to hypercoordination is a driving force for somewhat weaker dative bonding to the  $SiF_3$  group in **6b**.

Complexation of the silenes to **6a'** via only the N→Si dative bond  $BF_2CH_2NMe_2 \rightarrow H_2Si=CH_2$  and  $SiF_3CH_2NMe_2 \rightarrow H_2Si=CH_2$  resulted in  $n$ -donor complexes **10a** and **10b**, which are 40.4 and 20.1 kcal/mol less stable than the corresponding ditopic complexes **7a** and **7b**. Despite the lesser stability of  $n$ -donor complexes **10** and **11** their optimization never reached rearrangement into the ditopic complexes **7** and **8**. Also we checked whether complexation of silenes to **6a'** and **6b** via the only C→B or C→Si dative bond may compete with the ditopic complexation, giving products that are more stable than **7** and **8**. The attempted modeling of the  $H_2Si=CH_2 \rightarrow BF_2CH_2NMe_2$  and  $Me_2Si=CH_2 \rightarrow BF_2CH_2NMe_2$  complexes resulted in the products of silene insertion into the B–F bond of **6a'**, i.e., *trans*- $H_2FSiCH_2BFCH_2NMe_2$  (**12a**) and *trans*- $Me_2FSiCH_2BFCH_2NMe_2$  (**13a**). At that, **12a** appeared to be by 2.2 kcal/mol less stable than **7a**, but **13a** was 1.4 kcal/mol more stable than **8a**. Hence, ditopic complexation of parent silene to **6a'** should not be suppressed by the competitive insertion into the B–F bond in **6a'**, but it might be opposite in the case of dimethylsilene. The dimerization of **6a'** (dimerization energy −56.7 kcal/mol)

(29) For all the bonds a fluctuation of the population,  $\sigma^2/N$ , is below the unit characterizing the well-localized two-center bonds.

(30) Gruetzmacher, H.; Faessler, T. F. *Chem.–Eur. J.* **2000**, *6*, 2317.

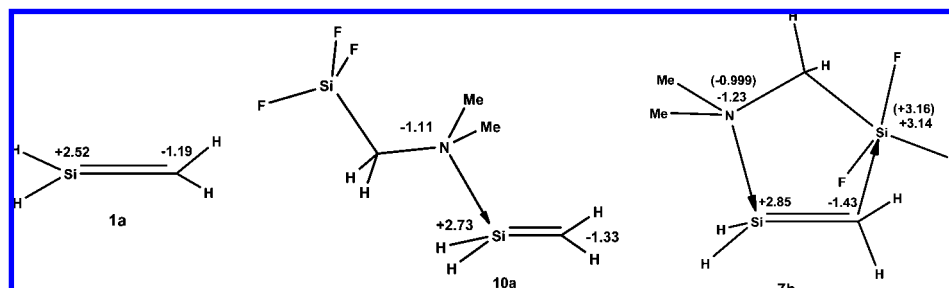


**Figure 10.** Selected AIM charges in silene and its *n*-donor and ditopic complexes. Charges in the free ligand are given in parentheses.

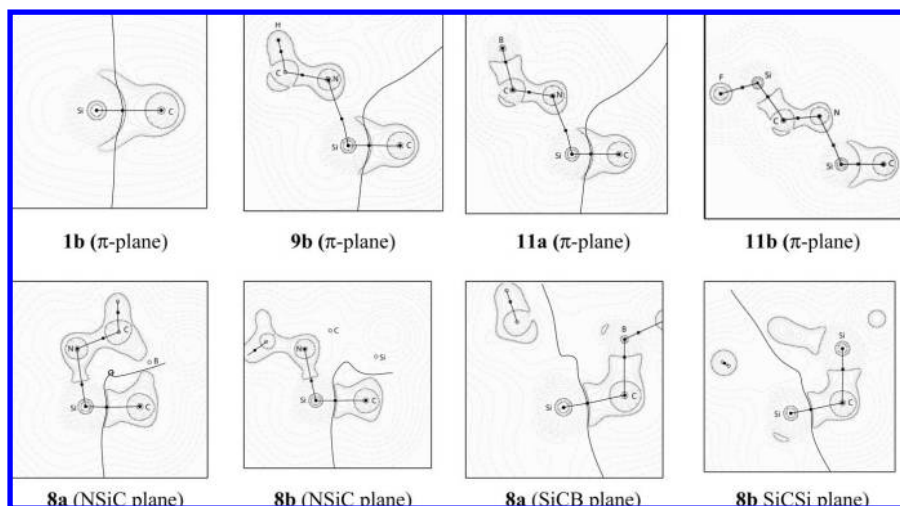


**Figure 11.** Laplacian maps for dimethylsilene and its *n*-donor and ditopic complexes. The diagrams are superimposed with the selected bond paths. Critical points (3, −1) are denoted by solid squares. Dashed lines correspond to  $\nabla^2\rho(\mathbf{r}) > 0$  (regions of charge depletion) and solid lines to  $\nabla^2\rho(\mathbf{r}) < 0$  (regions of charge concentration). The contour values in  $e/a_0^5$  are  $\pm 0.002$ ,  $\pm 0.004$ , and  $\pm 0.008$ .

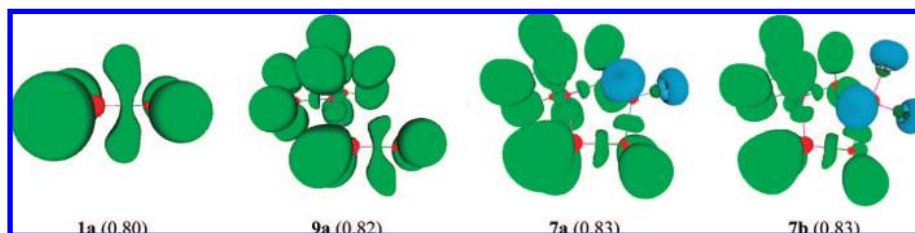


**Figure 12.** Localization domains of silene and its *n*-donor and ditopic complexes as shown by ELF (isosurfaces are given in parentheses). Green demonstrates the disynaptic binding basins, and light green is the disynaptic basins, surrounding hydrogen atoms. Red shows the spanning basins of silicon and skeleton atoms. Monosynaptic basins of lone pairs of the fluorine atoms are denoted by blue.

may also hinder its ditopic coordination to the parent silene, whereas no competition is expected for ditopic coordination of silicon-containing ligand **6b** to both silenes **1a** and **1b** owing to the very low dimerization energy of **6b** (−4.5 kcal/mol). Optimization of the complex formed with the only C→Si dative bond,  $\text{H}_2\text{Si}=\text{CH}_2 \rightarrow \text{SiF}_3\text{CH}_2\text{NMe}_2$ , formed the weak van der Waals complex **14**. Therefore, ditopic complexes **7b** and **8b** of silenes with silicon-containing ligand **6b** may be considered as the most experimentally obtainable ones, which is also supported by the synthetic availability of **6b**. Moreover, in this paper we predicted the possibilities of varying structure and energetics as well as the redistribution of  $\pi$ -electron density between the silenic fragment and dative C→Si bonds to give the most stable complex with the most preserved identity of silene's double bond (see Appendix).

The structures of the ditopic complexes are the five-membered rings in a semi-chair conformation. The N→Si bonds in **7** (1.934 and 1.964 Å) and in **8** (1.943 and 1.943 Å) are shorter than

those in the *n*-donor complexes **9–11** (2.149–2.268 Å) but still 11.3–12.9% longer than the covalent N→Si bonds in **3** (1.737–1.74 Å). The dative C→B bonds in **7** (1.662 and 1.652 Å) are ~7% longer than the covalent C→B bond in **3a** (1.547 Å). In turn, the dative C→Si bonds in **8** (2.015 and 1.910 Å) are 10% and 4% longer than the covalent C→Si bond in **3b** (1.833 Å). The SiC bonds in **7** (1.827 and 1.812 Å) and **8** (1.834 and 1.823 Å) are substantially longer than those in silene and dimethylsilene (1.716 and 1.714 Å) but obviously shorter than the single Si→C bonds in **3a** (1.908 and 1.904 Å) and **3b** (1.889 and 1.891 Å), indicating a partially doubly bonded silenic moiety in the ditopic complexes.

AIM topological analysis of the electron density distribution in **7** and **8** reveals bond critical points of (3, −1) rank in the interatomic areas of all the bonds including dative ones. A ring critical point of (3, +1) rank found approximately in the center of the five-membered fragments NSiCBC and NSiCSiC is definitely indicative of the cyclic structures of **7** and **8**. Both



**Table 7. Volume,  $V$ , Mean Population,  $N$ , and Dispersion,  $\sigma^2$ , for the Valence Mono- and Disynaptic Basins of Silene and Its  $n$ -Donor and Ditopic Complexes**

molecule or complex	basin	$V$	$N$	$\sigma^2$
<b>1a</b>	V1(Si <sup>1</sup> ,C)	113.56	1.87	0.99
	V2(Si <sup>1</sup> ,C)	113.07	1.77	0.95
<b>1b</b>	V1(Si <sup>1</sup> ,C)	107.74	1.95	1.00
	V2(Si <sup>1</sup> ,C)	106.14	1.77	0.95
<b>7a</b>	V(Si <sup>1</sup> ,C)	45.45	2.05	1.01
	V(Si <sup>1</sup> ,N)	27.84	2.15	1.07
	V(B,C)	24.20	1.81	0.96
<b>7b</b>	V(Si <sup>1</sup> ,C)	46.89	2.12	1.04
	V(Si <sup>1</sup> ,N)	27.60	2.13	1.06
	V(Si <sup>2</sup> ,C)	26.92	1.81	0.96
<b>8a</b>	V(Si <sup>1</sup> ,C)	41.09	2.06	1.02
	V(Si <sup>1</sup> ,N)	28.80	2.17	1.07
	V(B,C)	24.50	1.91	0.97
<b>8b</b>	V(Si <sup>1</sup> ,C)	38.56	2.01	1.01
	V(Si <sup>1</sup> ,N)	27.46	2.15	1.06
	V(Si <sup>2</sup> ,C)	34.89	1.94	0.98
<b>9a</b>	V1(Si <sup>1</sup> ,C)	103.86	1.89	0.99
	V2(Si <sup>1</sup> ,C)	64.10	1.79	0.98
	V(Si <sup>1</sup> ,N)	26.71	2.13	1.06
<b>9b</b>	V1(Si <sup>1</sup> ,C)	95.37	1.86	0.99
	V2(Si <sup>1</sup> ,C)	56.65	1.86	1.02
	V(Si <sup>1</sup> ,N)	28.89	2.16	1.07
<b>10a</b>	V1(Si <sup>1</sup> ,C)	103.21	1.86	0.98
	V2(Si <sup>1</sup> ,C)	62.94	1.85	1.00
	V(Si <sup>1</sup> ,N)	26.23	2.10	1.06
<b>10b</b>	V1(Si <sup>1</sup> ,C)	102.93	1.86	0.98
	V2(Si <sup>1</sup> ,C)	63.79	1.84	1.00
	V(Si <sup>1</sup> ,N)	26.48	2.11	1.06
<b>11a</b>	V1(Si <sup>1</sup> ,C)	94.91	1.87	1.00
	V2(Si <sup>1</sup> ,C)	55.38	1.85	1.03
	V(Si <sup>1</sup> ,N)	28.78	2.16	1.06
<b>11b</b>	V1(Si <sup>1</sup> ,C)	92.46	1.86	0.98
	V2(Si <sup>1</sup> ,C)	55.48	1.88	1.03
	V(Si <sup>1</sup> ,N)	28.57	2.15	1.06

**Table 8. Properties of the Si=C and C→Si Bond Critical Points in Ditopic Complex 15<sup>a</sup>**

Si=C			C→Si	
$\rho(\mathbf{r})$	$\nabla^2\rho(\mathbf{r})$	$\epsilon$	$\rho(\mathbf{r})$	$\nabla^2\rho(\mathbf{r})$
0.911	8.408	0.19	0.368	0.167

<sup>a</sup>  $\rho(\mathbf{r})$ , charge density at the BCP in  $\text{e}/\text{\AA}^3$ ;  $\nabla^2\rho(\mathbf{r})$ , Laplacian of  $\rho(\mathbf{r})$  at the BCP in  $\text{e}/\text{\AA}^5$ ;  $\epsilon$ , ellipticity.

**Table 9. Volume,  $V$ , Mean Population,  $N$ , and Dispersion,  $\sigma^2$ , for the Valence Disynaptic Basins in Ditopic Complex 15**

basin	$V$	$N$	$\sigma^2$
V(Si <sup>1</sup> ,C)	62.44	2.23	1.10
V(Si <sup>1</sup> ,N)	25.64	2.13	1.05
V(Si <sup>2</sup> ,C)	30.47	1.59	0.92

values of the electron density at the BCP and Laplacian are characteristic of polar covalent N→Si, C→B, and C→Si bonds. In contrast to the  $n$ -donor complexes **9**–**11**, where the electron densities at the BCP of the silenic moiety are close to  $\sim 0.96 \text{ e}/\text{\AA}^3$ , in **7a** and **8a** they are reduced to 0.88 and 0.89  $\text{e}/\text{\AA}^3$ , respectively. A somewhat different nature of the Si=C bond emerges from the ELF analysis, indicating the only valence disynaptic basin in interatomic area between silicon and carbon in the silene moiety of ditopic complexes **7** and **8**. Its volume and mean population rather resemble the ordinary SiC bond. Therefore, one may conclude that both dative C→B and C→Si bonds are formed by accepting a considerable portion of the silene's  $\pi$ -electron density by boron and silicon, respectively.

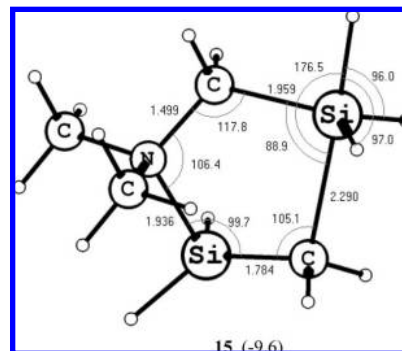
Unlike methylene-bridged ligands, which turned out appropriate for the optimization of ditopic silene complexes, attempted modeling of the complexes with ligands containing no or two

methylene groups resulted in the insertion products  $\text{Me}_2\text{NR}_2\text{SiCH}_2\text{X}$  and  $\text{R}_2\text{FSiCH}_2\text{XCH}_2\text{CH}_2\text{NMe}_2$ , respectively.

Finally, the relationship between kinetic stability of ditopic complexes and the double-bond character of the Si=C bond is worthy of note. Kinetic stability of the complexes to cyclo-dimerization may include the stage of the complex dissociation.<sup>21</sup> Therefore, one can expect that the higher the complexation energy, the more stable the Si=C double bond in the complex. This assumption has experimental support.<sup>5a</sup> However, an increase of the complexation energy inevitably results in the lowering of the Si=C double-bond character. Thus, according to the results of the calculations, a silenic moiety in the complexes **7a** and **8a** with boron-containing ligands is characterized by its low double-bond character. Ditopic complexes **7b** and **8b** formed by silicon-containing ligands maintain their double-bond character in somewhat higher degree. In other words, silenic moieties conserve to some degree their chemical identity. Therefore, one may conclude that ditopic complexes should react like simple unprotected silenes but with a substantially higher activation energy.

## Appendix

Here we report the possibility of managing the degree of double bonding in the silenic fragment of the ditopic complexes with organosilicon ligands. Thus, the doubly bonded character of the silicon–carbon bond in the silenic moiety of the ditopic complexes could be increased by reducing the acceptor ability of the silyl group by replacing fluorine in **6b** with hydrogen. A preliminary ab initio study of silene complexation to a (dimethylaminomethyl)silane ligand resulted in ditopic complexes **15**, whose structure and complexation energy are given below.



It is seen that the silicon–carbon bond in the silene moiety of **15** became 0.039  $\text{\AA}$  shorter than that in **7b**. On the contrary, the dative C→Si bond is elongated by 0.297  $\text{\AA}$ . Such a change in geometries on going from **7b** to **15** resulted in a decrease in complexation energy from  $-27.3$  to  $-9.6 \text{ kcal/mol}$ , due to the redistribution of  $\pi$ -electron density between the silenic fragment and dative C→Si bonds. The topology of the electron density distribution in terms of AIM and ELF theories is given in Tables 8, 9 and Figures 13, 14.

The AIM analysis data are indicative of partial retention of the double SiC bond in **15**. Indeed, though the ellipticity value in its BCP (3,–1) is inferior to that of the parent silene **1a** (by  $\sim 37\%$ ), it is nearly twice as large as  $\epsilon$  in complex **7b** (see Tables 6 and 8). With respect to **7b** a charge density at the Si=C BCP,  $\rho(\mathbf{r})$ , is increased in **15** by 0.02  $\text{e}/\text{\AA}^3$ , whereas for the dative C→Si bond it substantively lowers by 0.256  $\text{e}/\text{\AA}^3$  (41%). Electron density is mainly localized within silenic moiety **15** (Figure 13); as in the case of the parent silene **1a**, it does not completely belong to the carbon basin, because its “lug”, which

Chart 1

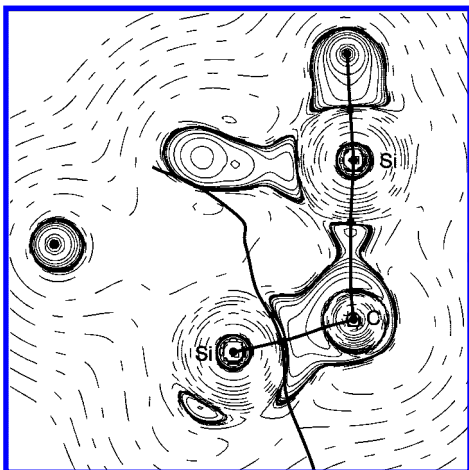
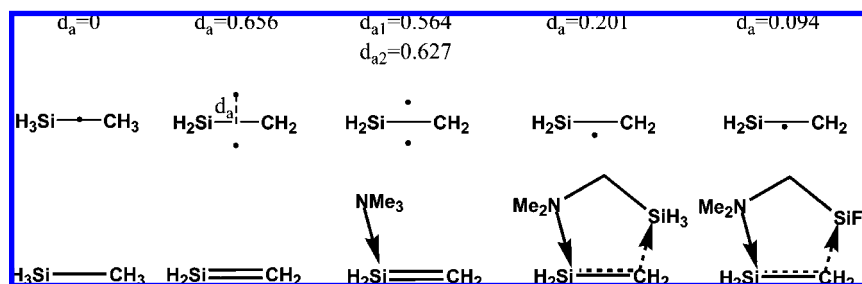


Figure 13. Laplacian map by AIM theory for ditopic complex 15.

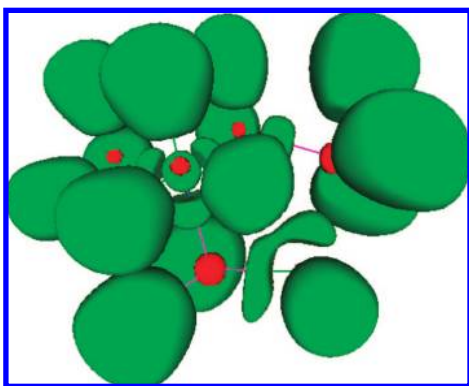


Figure 14. ELF localization domains (0.83) for ditopic complex 15.

is also located in the atomic region of the silene's Si atom, is well seen under the plane of the  $\pi$ -bond.

A similar electron distribution emerges from ELF localization domains shown in Figure 14. It is seen that  $\pi$ -electron density remaining in the silenic moiety is also involved into the formation of the dative  $C \rightarrow Si$  bond. Correspondingly, the ELF topology of **15** reveals that the volume of the disynaptic basins

of silenic bond  $V(Si^1, C)$  as well as the population is increased by 33.2% with regard to **7b** (see Tables 7, 9).

In the case of **7b** the "dumbbell", which characterizes a normal double bond in ELF analysis in **1a** and **9a** (Figure 14), has been split into two disynaptic basins (ELF = 0.83). On the contrary, in **15** its form is substantially changed (the top of the dumbbell is withdrawn into the region of the dative  $C \rightarrow Si$  bond), but no splitting of the dumbbell is observed. This, undoubtedly, is indicative of partial retention of the  $Si=C$  double-bond character in ditopic complex **15**.

In Chart 1, the ELF maxima and their position with respect to the interatomic vector ( $d_a$ , Å) for bonds SiC in methylsilane, silene, and complexes **9a**, **15**, and **7b**, respectively, are shown.

It is seen that for methylsilane the ELF maximum is located on the Si-C interatomic vector, whereas for the parent silene two maxima above and below the vector are separated by the minimum on it. In the case of **7b** the ELF maximum holds the position almost like it does in methylsilane, whereas in **15** there is only one maximum shifted below the  $Si=C$  bond vector, which also points at its partial double-bond character.

Therefore, changing substituents at the acceptor atoms of the ligand can tune the degree of the double-bond character in silene moieties in ditopic complexes.

**Acknowledgment.** This paper is published in commemoration of Prof. Leonid E. Gusel'nikov, whose contribution to the chemistry of silenes was fundamental. Prof. T. J. Barton's assistance in correcting the final version of the manuscript is highly appreciated. Financial support from the International Association for the Promotion of Cooperation with Scientists from the New Independent States of the Former Soviet Union (Grant INTAS 03-51-4164) and from the Russian Foundation for Basic Research (Grant RFBR No. 06-03-32559) is gratefully acknowledged.

**Supporting Information Available:** Tables of total energies, zero-point energies,  $E_0$ , enthalpies of complexation and addition reactions, and geometric parameters of silenes, ligands, adducts, and  $n$ -donor complexes, Cartesian coordinates of **6**, **7**, **8**, **15**, and  $Me_2NCH_2SiH_3$ . This material is available free of charge via the Internet at <http://pubs.acs.org>.

OM800243J